Chemical Engineering Science 154 (2016) 20–26

Contents lists available at ScienceDirect

Chemical Engineering Science

journal homepage: www.elsevier.com/locate/ces

Scalable solvo-plasma production of porous tin oxide nanowires

Tu Quang Nguyen [a,b,c], Veerendra Atla [a,b], Venkat Kalyan Vendra [a,b], Arjun Kumar Thapa [a], Jacek Bogdan Jasinski [a], Thad Lawrence Druffel [a], Mahendra Kumar Sunkara [a,b,*]

[a] Conn Center for Renewable Energy Research, University of Louisville, Louisville, KY 40292, United States
[b] Department of Chemical Engineering, University of Louisville, Louisville, KY 40292, United States
[c] Advanced Energy Materials, LLC, Louisville, KY 40299, United States

HIGHLIGHTS

- A fast (reaction time scale less than 1 min), scalable method for synthesizing tin oxide nanowire powder using atmospheric plasma.
- The mechanism for observed one-dimensional growth is explained through the observation of an intermediate phase involving potassium stannate.
- The conversion of potassium stannate nanowires through acid wash followed by simple annealing step resulted in porous tin oxide nanowires.
- The resulting porous tin oxide nanowire powder shows a high reversible capacity of 848 mA h g^{-1} after 55 cycles at a current density of 100 mA g^{-1}.
- A large-scale production of tin oxide nanowire powder as high as 10 g per hour has been produced and could be increased further up to 300 g per hour using a lab-scale roll-to-roll setup.

GRAPHICAL ABSTRACT

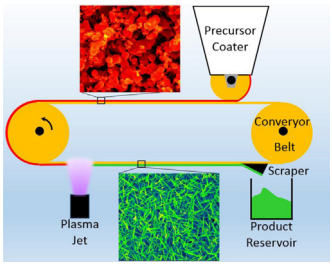

ARTICLE INFO

Article history:
Received 19 December 2015
Received in revised form
28 February 2016
Accepted 4 March 2016
Available online 22 March 2016

Keywords:
Tin oxide nanowires
Porous nanowires
Roll-to-roll
Scalable

ABSTRACT

This paper reports a fast, scalable method for synthesizing tin oxide nanowire powder using cheap starting material of commercial tin oxide particles and an atmospheric microwave plasma reactor. Specifically, the synthesis concept involves plasma oxidation of tin oxide powder combined with potassium hydroxide for few seconds to a minute which is orders of magnitude lower than that using hydrothermal or vapor–liquid–solid (VLS) techniques. Even at lab scale, large-scale production of tin oxide nanowire powder as high as 10 g per hour has been produced. Systematic studies reveal nucleation and growth of K_2SnO_3 nanowires from molten alloy involving KOH and tin oxide. A simple annealing step is used to convert K_2SnO_3 intermediate nanowires into pure tin oxide nanowires. The extremely short reaction time of 20 s is three orders of magnitude faster than that of traditional hydrothermal method. It was shown that our tin oxide nanowire powder shows a high reversible capacity of 848 mA h g^{-1} after

* Corresponding author at: Conn Center for Renewable Energy Research, University of Louisville, Louisville, KY 40292, United States.
E-mail address: mahendra@louisville.edu (M.K. Sunkara).

http://dx.doi.org/10.1016/j.ces.2016.03.008

Large quantities
Li-ion batteries

55 cycles at a current density of 100 mA g^{-1}. The scalable production technique presented here and the applicability of resulting tin oxide nanowire powders makes it as suitable for practical implementation into lithium-ion battery applications.

1. Introduction

Tin oxide nanowires is one of the most promising 1D nanostructures for advanced applications in lithium-ion batteries (Meduri et al., 2009), solar cells (Gubbala et al., 2009), sensors (Hui et al., 2006), optical devices (Chandra et al., 2008), and electronic devices(Kolmakov et al., 2008). However, the wide-spread use of nanowire based materials in to energy device applications has been limited due to the fact that there are no scalable manufacturing methods, yet. For example, the lithium-ion battery electrodes will require production on the order of kilograms even for simple pouch cell prototyping. Thus, the development of reliable, reproducible and simple techniques for production of tin oxide nanowires and their testing into energy devices is of great interest. Up to date, several approaches have been proposed to prepare tin oxide nanowires including chemical vapor deposition (Dai et al., 2002), laser ablation (Liu et al., 2003), template method (Zhang et al., 2011) and most predominantly hydrothermal technique (Wang et al., 2003).

Hydrothermal synthesis has been traditionally used to prepare nanostructured materials including nanoparticles and nanowires. However, this approach requires long time scale, high pressure, multiple steps and expensive precursors (Zhang et al., 2006). Further, in most cases, hydrothermal techniques require the use of surfactant to control the nanowire growth. Also, no clear mechanism for tin oxide nanowires have been proposed. Importantly, the hydrothermal techniques are limited to lab scale (few milligrams to hundred milligrams a batch) (Cheng et al., 2004; Jian et al., 2003). Two recent hydrothermal based approaches are microwave assisted hydrothermal and continuous flow hydrothermal method, which can increase the production rate to about 5 g/day and 10 g/h, respectively (Cabanas et al., 2000; Chung et al., 2008). However, these hydrothermal methods have been shown to work only for nanoparticles (NPs) and not to make nanowires. Another popular method for making nanowire growth is that using vapor–liquid–solid (VLS) process for many semiconductors including tin oxide (Dai et al., 2002). However, VLS processes require the use of low pressure, high temperatures, high fabrication cost and Au as catalyst.

In this work, we report a facile, fast "solvo-plasma" production of tin oxide nanowires using tin oxide particles as a low-cost source. This study demonstrates, for the first time, the direct conversion of tin oxide particles to tin oxide nanowires with reaction time scales on the order of a minute or lower. More importantly, various experimental studies are used to understand the underlying principle of nucleation and growth of tin oxide nanowires in the presence of alkali hydroxides. Thin films made using the resulting tin oxide nanowire powders are also investigated for their performance as high capacity anodes in lithium ion batteries.

2. Experimental

Tin oxide nanowires are synthesized in an upstream microwave plasma reactor whose details have been described in detail elsewhere (Kumar et al., 2011). Briefly, tin oxide particles ($1 \div 5$ μm size, Atlantic Equipment Engineer, Inc) are mixed with KOH powder in a 3:1 ratio by weight and water is added to make the precursor paste. The precursor paste is then sprinkled on the top of a 1×1 in. quartz substrate (Fig. 1a), which is then carefully exposed to the plasma flame at power of 1.0–1.4 kW, 8 l pm of Air flow for 10 s to 5 min. The as-synthesized materials are dispersed in 0.1 M HCl solution for 1 h to facilitate ion exchange, washed with deionized water, and annealed by exposure to plasma flame for 1–5 min. The samples are characterized using a scanning electron microscope (SEM) (FEI Nova 600), X-ray diffraction (Bruker D8 Discovery with Cu Kα radiation), and a transmission electron microscope (TEM) (Tecnai F20 FEI TEM operating at 200 kV).

The electrochemical measurements are performed using a battery tester (16 Channel Arbin Instruments, USA). The electrode materials were prepared using 70 wt% active materials with 20 wt% AB (acetylene black) and 10% PVDF binder in NMP. The well-mixed slurry was casted onto a copper foil using a doctor blade. The electrode is dried at 180 °C for 4 h under vacuum. The typical loading of active materials is 0.2–0.5 mg/cm^2. The CR-2032 coin-type assembling is performed in a dry argon-filled glove box. The electrodes are separated by two pieces of glass fiber filter. The electrolyte solution was 1 M $LiPF_6$–EC:DMC (1:2 by volume).

3. Results and discussion

All experiments are performed using inexpensive, commercial tin oxide particles without any further purification by mixing them with KOH and exposing to atmospheric plasma flame for 15 s to 1 min. Using a 1-in. square substrate, we were able to demonstrate production of tin oxide nanowires at a scale of 10 g in one hour (Fig. 1b). The exposure time used here is less than a minute which is about 3.5 orders of magnitude faster than that using a hydrothermal method. Fig. 2a shows SEM images of the resulting tin oxide nanowires that are 2 μm in length and about 50–100 nm

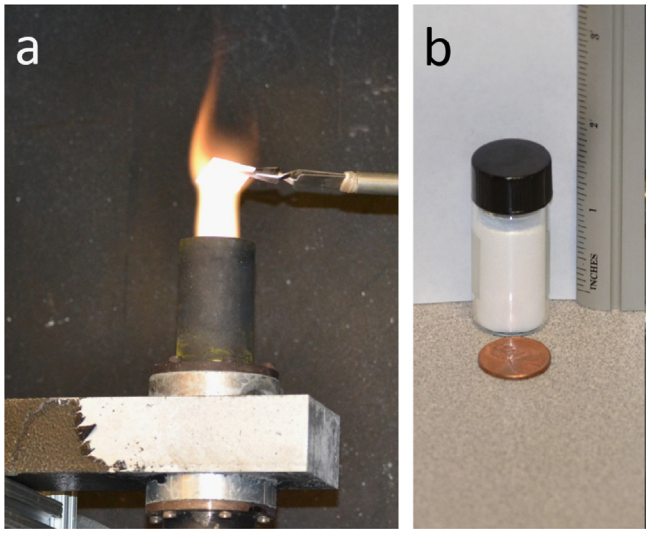

Fig. 1. Photograph of an actual experiment: plasma exposure of tin oxide precursor and KOH paste on quartz substrate a), a bottle of tin oxide nanowire powder of 10 g produced in one hour reaction time.

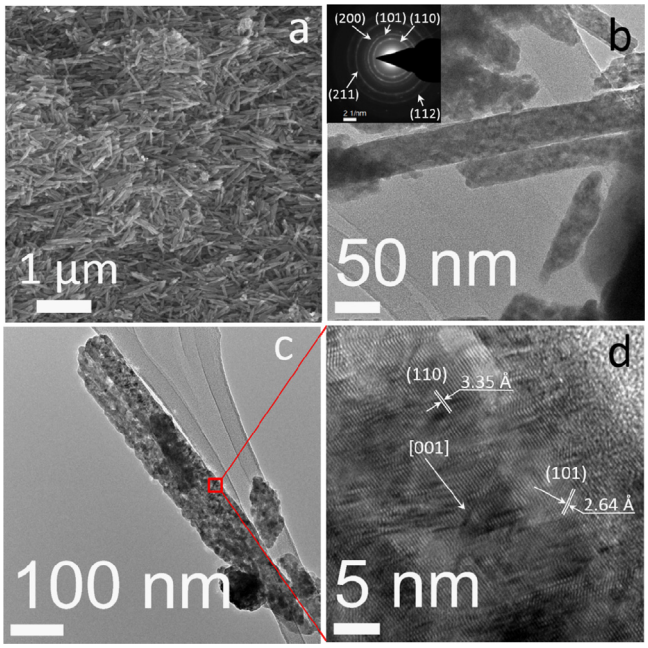

Fig. 2. Scanning electron microscopy of tin oxide nanowire powder after annealing a), TEM images b) and c) showing the porous structure and twining effect, (inset) SAED of tin oxide nanowires, HR-TEM image showing the matching interplanar lattice spacing of (110) and (101) plane of tin oxide nanowires d).

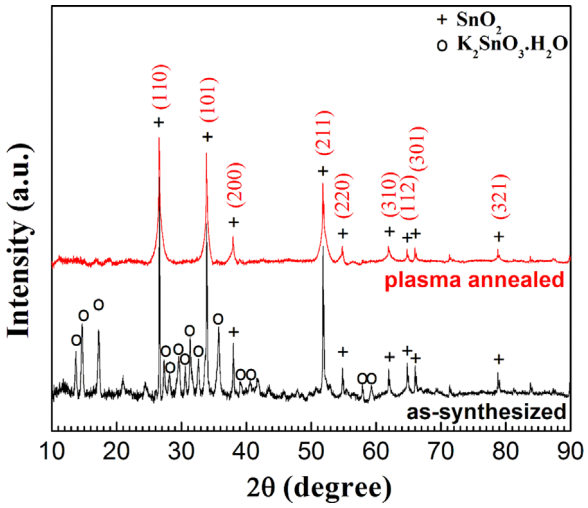

Fig. 3. Powder XRD pattern of samples after annealing in plasma showing the pure phase of rutile tin oxide while the as-synthesized samples showing additional intermediate compounds.

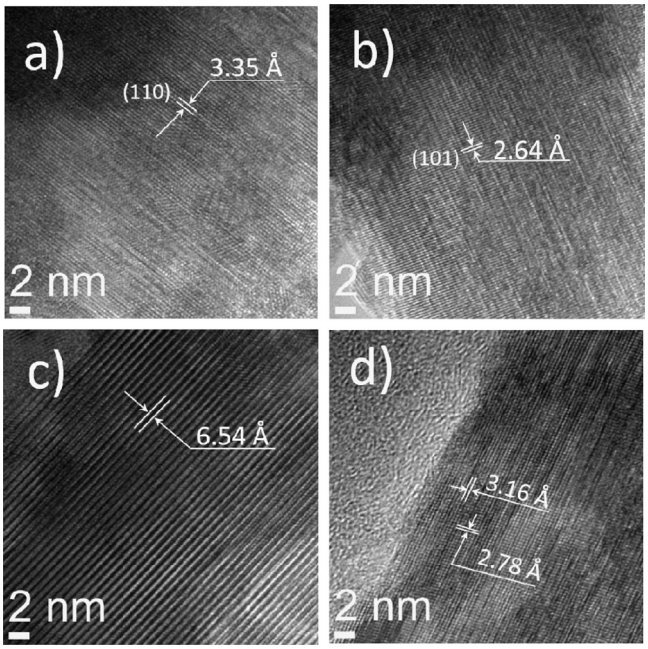

Fig. 4. HR-TEM images of as-synthesized samples showing well-matched interplanar lattice spacing of rutile tin oxide in (a) and (b), $K_2SnO_3 \cdot H_2O$ in (c) and (d).

in diameter. The TEM images of tin oxide nanowires show highly porous structures of tin oxides, which is due to HCl ion exchange and plasma annealing step (Fig. 2b, and c). The BET surface area of the porous tin oxide nanowires turned out to be 37 m^2/g. The BET surface area could be increased further by controlling the ion exchange and annealing parameters. The phase transformation of intermediate nanowires to tin oxide nanowires created the porous structures where potassium and water vapor are removed. The porous structures consisted of interconnected tin oxide nanoparticles. The underlying mechanism for porous structure formation seems to be similar to that suggested in many other reports using hydrothermal synthesis with additional annealing step (Wang et al., 2003). However, the actual mechanism is not completely clear in terms of how phase transformation leads to porous nature within the nanowires. Fig. 2c also revealed the twining effect where the boundary in the top left corner clearly showed merging of two nanowires. The merging maybe due to the high surface diffusion of tin atoms on nanowire surface under plasma exposure (Ostrikov et al., 2010). The HR-TEM image in Fig. 2d shows the match of interplanar lattice spacing of 3.35 Å and 2.64 Å for the plane (110) and (101), respectively.

The powder XRD pattern of tin oxide nanowires after annealing in plasma is shown in Fig. 3. The diffraction peaks revealed that tin oxide nanowires have tetragonal crystal structure with lattice parameters $a=b=4.74$ Å and $c=3.18$ Å, corresponding bulk rutile tin oxide (PDF-00-005-0467). The selected area diffraction pattern also confirms the pure phase tin oxide as in Fig. 2b. No other impurity peaks are detected in the tin oxide nanowire samples after annealing in plasma. The Raman spectroscopy of the tin oxide nanowires after annealing shows fundamental peaks at 474, 633, and 775 cm^{-1} that is well matched with rutile tin oxide (Zhou et al., 2006) (Fig. S1). In addition to the peaks of tin oxide phase, the XRD pattern of as-synthesized samples (Fig. 3) showed peaks of $K_2SnO_3.H_2O$ (PDF-00-019-0993). The HR-TEM images showed well-matched interplanar lattice spacing of SnO_2 (Fig. 4a, and b) and layered structure $K_2SnO_3 \cdot H_2O$ (Fig. 4c, and d). The lattice spacing of 6.54 Å, 3.16 Å and 2.78 Å correspond to the peaks of 13.5°, 28.2°, and 32.2° of $K_2SnO_3 \cdot H_2O$. EDS analysis shows that the as-synthesized nanowires contain about 13 at% of potassium. This confirms that the intermediate compound or as-synthesized compound is K_2SnO_3. The hkl index of $K_2SnO_3 \cdot H_2O$ is not available to our knowledge. However, the lattice spacing of tin oxide in Fig. 2d shows that tin oxide nanowires grown along [001] direction that is in agreement with previous reports (Zhang et al., 2006; Wang et al., 2004). [001] Direction has highest surface energy that favored the 1D growth (Cheng et al., 2004; Beltrán et al., 2003).

Even though, the above results clearly demonstrate the formation of one-dimensional structures with plasma exposure of tin oxide powder mixed with KOH, there are several questions remain unanswered about the observed 1-D growth. So, experiments were conducted for different weight ratios of SnO_2 to KOH to

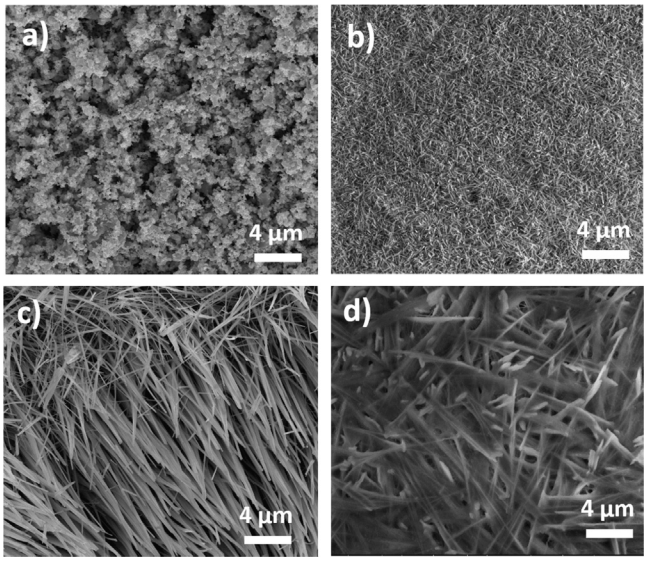

Fig. 5. SEM images of (a) tin oxide precursor and as-synthesized K_2SnO_3 nanowires at weight ratios of SnO_2 to KOH of (b) 3:1, (c) 1:1, (d) 1:3. Experiments were conducting using plasma flame with power of 1.2 kW at a duration of 60 s.

understand initial stages of growth. Fig. 5 shows the SEM images of as-synthesized samples at different weight ratios of SnO_2 to KOH in comparison with the tin oxide particle precursor. Thin, short nanowires of about 70 nm in diameter and 2 to 4 μm in length are observed at weight ratio of 3 to 1. When the weight ratio for precursors decreased to 1–1, there is more change in the nanowire diameter and length. As shown in Fig. 5c, the resulting nanowires are of 100–300 nm in diameter and 20–30 μm in length. The image also shows that nanowires bunch up and seem to be fusing together for samples grown using precursors at a weight ratio of 1 to 1. Such sintering of nanowires could be the reason for twining effect seen in Fig. 2c. The nanowire diameter increased further when using precursor ratio to 1:3. However, there is the presence of excess KOH on top of nanowires that make it difficult to quantify diameters. The increase in diameter for resulting nanowires can probably be explained with decreasing supersaturation with decreasing SnO2 to KOH ratio from 3:1 to 1:3.

Experiments were also performed using different tin precursors such as tin oxide, tin and tin monoxide to determine their impact on reaction time scales and nanowire growth rates. As shown in Fig. 6, K_2SnO_3 nanowires are obtained using a mixture of tin metal powder or tin mono-oxide particles with KOH. Nanowires obtained using tin metal powder have random diameters and lengths. Nanowires obtained using tin mono-oxide have diameters of about 50–100 nm and lengths up to 50 μm (Fig. 6d). In fact, tin oxide nanoparticles are always found together with K_2SnO_3 nanowires when tin metal powder used as starting material (Fig. 6b, and c). No nanowires formed with either mixture of H_2O or KCl with tin oxide particles (Fig. 6a). In another experiment, the same mixture of tin oxide particles and KOH at mass ratio of 3 to 1 is put onto a quartz substrate and was thermally heated to 900 °C for 2 h in a box furnace. The similar tin oxide nanowire morphology but longer in length is observed (Fig. 6f).

Based on all the experimental observations, we propose a mechanism to explain tin oxide nanowire growth in a three step sequence as shown in Fig. 7: (1) continuous dissolution of tin oxide particles with KOH results in supersaturation of tin oxide in molten phase containing K–Sn–O, (2) phase segregation and bulk nucleation of K_2SnO_3 on the surface of tin oxide particles due to non-stable molten phase containing K–Sn–O, (3) K_2SnO_3 formation started from surface of tin oxide particles by diffusion-driven self-

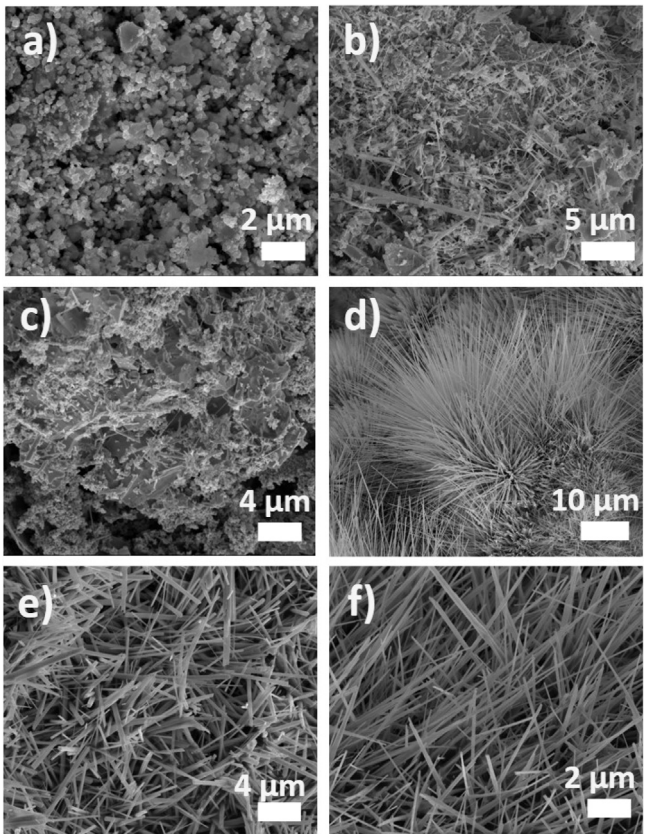

Fig. 6. SEM image of as-synthesized sample using a) SnO_2+KCl, b) Sn+KOH, c) Sn+KCl, d) SnO+KOH, e) K_2SnO_3, f) SnO_2+KOH. Sample a) to e) prepared using plasma heating for 60 s, sample f) prepared using thermal heating at 900 °C for 2 h.

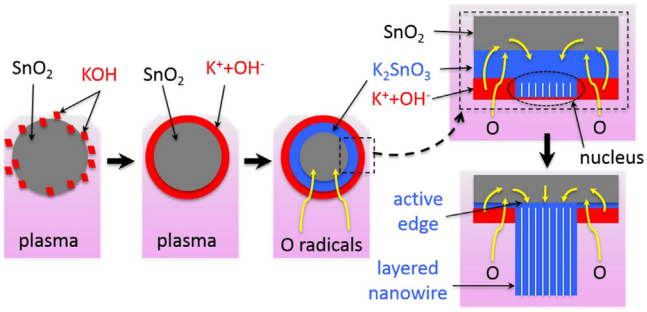

Fig. 7. Schematic showing the proposed growth mechanism for growth of tin oxide nanowires. a) Mixture of tin oxide particle and KOH in plasma flame, b) KOH got melted into free moving K^+ and OH^- ions, c) diffusion of oxygen radicals, K^+ and OH^- ions into tin oxide particle to form K_2SnO_3, d) K_2SnO_3 nucleus forming under supersaturation of K_2SnO_3, e) layered structure K_2SnO_3 grown due to active edge.

arrangement and basal attachment(Ostrikov et al., 2013). The resulting $K_2SnO_3 \cdot H_2O$ phase has layered structure with active sites at the edge sites for faster attachment kinetics. Faster growth kinetics along certain planes will only lead to platelet structure and morphology. So, in addition to faster growth kinetics at edges of layered structure, selective wetting of crystal nuclei with molten phase is hypothesized for ensuring one-dimensional growth for K_2SnO_3 nanowires. Extra exposure of K_2SnO_3 nanowires also result in tin oxide nanowires. So, the final product can contain pure tin oxide nanowires. But, based on our experimental data, the formation of K_2SnO_3 1-D structures occurs first and then transforms to pure phase tin oxide nanowires. Previous studies using hydrothermal method suggested that the formation of tin oxide

nanowires was due to decomposition of intermediate phase of $Na_2Sn(OH)_6$ to tin oxide nuclei followed by condensation to form tin oxide nanowires (Zhang et al., 2006; Qin et al., 2008).

In principle, KOH can easily be melted into free moving $K^+$and OH^- ions under plasma exposure or thermal heating up to 406 °C or higher. Indeed, an in-situ measurement of surface temperature using a Pyrometer which showed the temperature to be lower than its minimum detection limit of 475 °C after 17.4 s of exposure time. KOH probably melted sooner than 10 s of exposure time as shown in Fig. S2. Free moving $K^+$and OH^- ions and oxygen radicals(Davide and Sankaran, 2010; Mozetič et al., 2005) produced by atmospheric plasma flame quickly diffuse into tin oxide structure to form a thin layer of molten melted of K_2SnO_3 on the surface of tin oxide particles.

$$SnO_2+2K^++2OH^-+O\rightarrow K_2SnO_3+H_2O+1/2O_2\ \Delta G_{1,\ 900} \quad (1)$$

Fast diffusion of K^+, OH^- ions and oxygen radicals into tin oxide particles make tin oxide quickly dissolved to form a molten phase containing K, Sn and O in which the K_2SnO_3 phase forms and nucleates out. K_2SnO_3 is a layered structure itself in which the growth predominantly happens at its ends (at edge sites). The growth direction along the wide d-spacing of 6.54 Å was confirmed in all of the TEM analysis of the as-synthesized samples. Availability of $K^+$and OH^- ions make the edge, where nucleus is in contact with molten K_2SnO_3, is the only active edge that nucleus can propagate to form nanowire.

$$SnO_2+2K^++2OH^-\rightarrow K_2SnO_3+H_2O\ \Delta G_{2,\ 900} \quad (2)$$

Under thermal heating, the reaction (1) can be revised as shown in reaction (2). Under thermal heating up to 900 °C, KOH also became molten into free moving $K^+$and OH^- ions. The same growth mechanism can be applied in case of thermal heating. Gibbs free energy of K_2SnO_3 is not available yet. However, by assuming that the Gibbs free energy of K_2SnO_3 is a specific value of $X_{KSO,}$ then we could calculate Gibbs free energy change of above reactions at 900 °C. $\Delta G_{1,\ 900}$ and $\Delta G_{2,\ 900}$ are of $X_{KSO}+256.45$ and $X_{KSO}+432.84$ kJ. The difference of 176.39 kJ in Gibbs free energy indicates that presence of plasma makes the reaction (1) more spontaneous than reaction (2). Indeed, fast nanowire growth rate of 1 μm/min is observed with plasma heating while thermal heating resulted in slow nanowire growth rate of 0.04 μm/min. As a main specie of atmospheric plasma, highly active oxygen radicals (Mozetič et al., 2005) with K^+, OH^- ions diffuse quickly into tin oxide structure to form K_2SnO_3. Fast diffusion of oxygen radicals, K^+, and OH^- ions results in fast growth rate of nanowires in plasma heating.

$$SnO+2K^++2OH^-+O\rightarrow K_2SnO_3+H_2O\ \Delta G_{3,\ 900} \quad (3)$$

In another experiment, tin mono-oxide is used as starting material. The reaction occurs as reaction (3). The Gibbs free energy ($\Delta G_{3,\ 900}$) is calculated to be $X_{KSO}+87.75$ kJ which is 168.70 kJ lower than that of reaction (1) where tin oxide is used. As expected, the use of tin mono-oxide has increased the nanowire growth rate up to 40 μm/min that is 40 times faster than the use of tin oxide with plasma heating and 1000 time faster than the use of tin oxide with thermal heating.

$$Sn+2K^++2OH^-+2O\rightarrow K_2SnO_3+H_2O \quad (4)$$

The use of tin metal as starting material made a big difference. Tin metal can react directly with KOH to form K_2SnO_3 nanowires as reaction (4). Tin metal can also get oxidized to tin mono oxides, tin oxides and then these oxides react with KOH to form K_2SnO_3 nanowires. Therefore, random nanowire lengths are observed as tin mono-oxides tend to form long nanowire while tin oxides produce short nanowires. Several resulting tin mono-oxide or tin oxide particles, did not get in contact with KOH and are observed as particles in any experiments using tin metal as starting material.

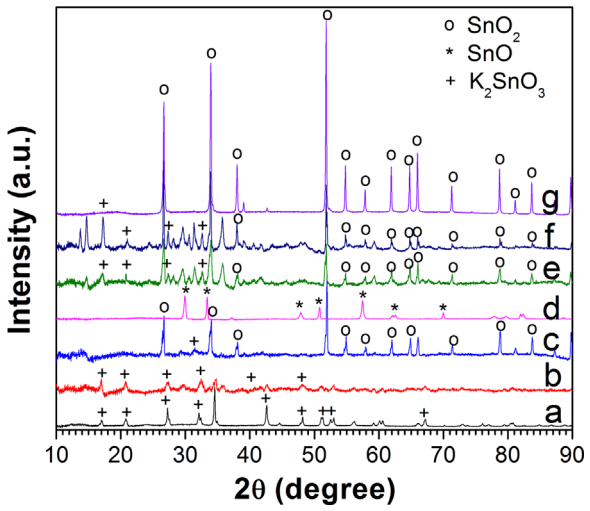

Fig. 8. XRD pattern of a) K_2SnO_3 particle precursor, b) as-synthesized nanowires using K_2SnO_3 particles, c) as-synthesized nanowires using tin mono oxide particles, d) tin mono oxide particle precursor, e) as-synthesized nanowires using tin oxide particles for 10 s exposure time, f) as-synthesized nanowires using tin oxide particles for 60 s exposure time, g) SnO_2 particle precursor.

The structure of as-synthesized nanowires using different starting materials for tin is investigated to understand the transformation of tin-based particle precursor to K_2SnO_3 nanowires. Fig. 8 shows the XRD pattern of as-synthesized nanowire samples using tin oxide, tin mono-oxide and K_2SnO_3 particles. Clearly, the nanowires prepared using K_2SnO_3 particles exhibit the same peaks of K_2SnO_3 phase as shown in Fig. 8a and b. Peaks of K_2SnO_3 appear in the samples prepared using tin oxide particles after 10 seconds of exposure time (see Fig. 8e). As the exposure time increased to 60 seconds, the intensity of these peaks increase significantly as shown in Fig. 8f. In other experiment with K_2SnO_3 particles as precursor, K_2SnO_3 remains the same phase but the morphology changes from particle form to nanowire form (Fig. 8a, and b and Fig. 6e). The formation K_2SnO_3 nanowires using K_2SnO_3 particles will be investigated for more detail in another study. The use of tin mono oxide as precursor does not show the formation of K_2SnO_3. As shown in Fig. 6d, the long nanowires prepared using tin mono oxide probably experience high temperature gradient and transform directly to tin oxide phase under plasma exposure. This is advantageous as it can further increase the production capacity of tin oxide nanowires using a roll-to-roll setup and expected to introduce a new commercial production of tin oxide nanowire powder for practical applications such as lithium ion batteries, solar cells. As shown in Fig. 9, the production capacity can be controlled by the thickness of precursor film, width of belt, speed of belt and plasma power. In our setup, the belt width of 2 in., the plasma power of 0.8–2.5 kW, belt speed of 1–2 in. per minute for exposure time of 30 s to 1 min, the precursor film thickness 100 μm to 1 mm. A simple calculation for plasma power of 1.5 kW, belt speed of 1 in. per minute, results in a production rate of 31–310 g/h for precursor thickness of 100 μm to 1 mm using estimated density of dried precursor film of 4 g/cm^3.

Availability of porous tin oxide nanowires in large quantities should be very interesting for prototyping applications in batteries, gas sensors and catalysts (Martinez et al., 2005). For lithium ion battery application, tin and its oxides are one of the most important anode materials due to their high volumetric capacity and decent gravimetric capacity of 7.25 A h cm^{-3} and 994 mA h g^{-1} for tin, 5.47 A h cm^{-3} and 781 mA h g^{-1} for tin oxide, respectively (Derrien et al., 2007; Winter and Besenhard, 1999). Moreover, nanowire

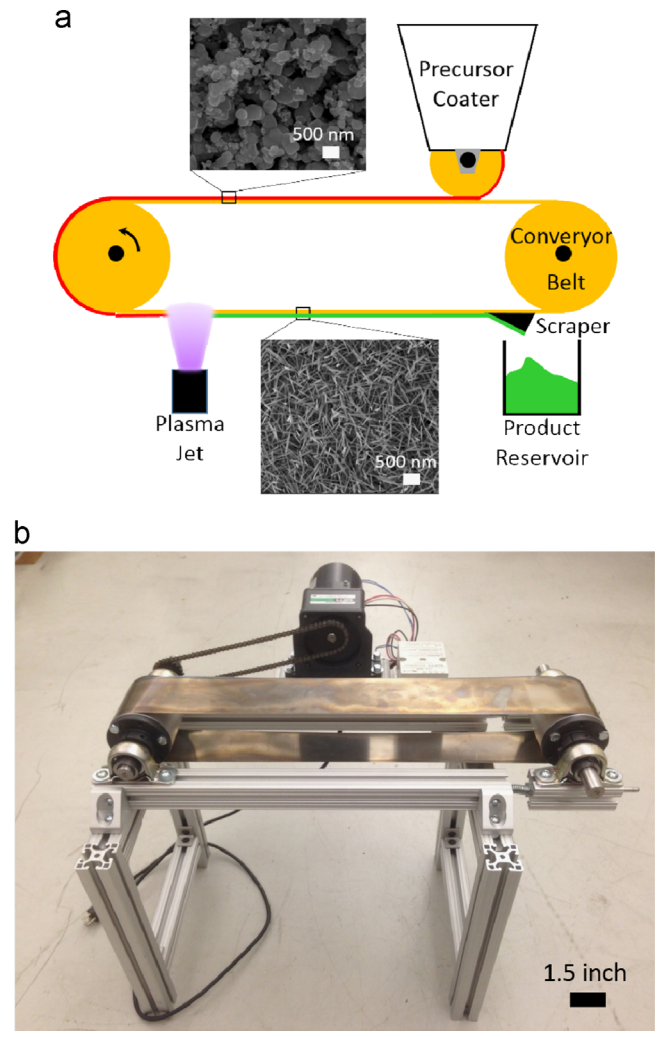

Fig. 9. a) Roll-to-roll setup for commercial production of tin oxide nanowire powder; b) A photo of lab-scale conveyor belt.

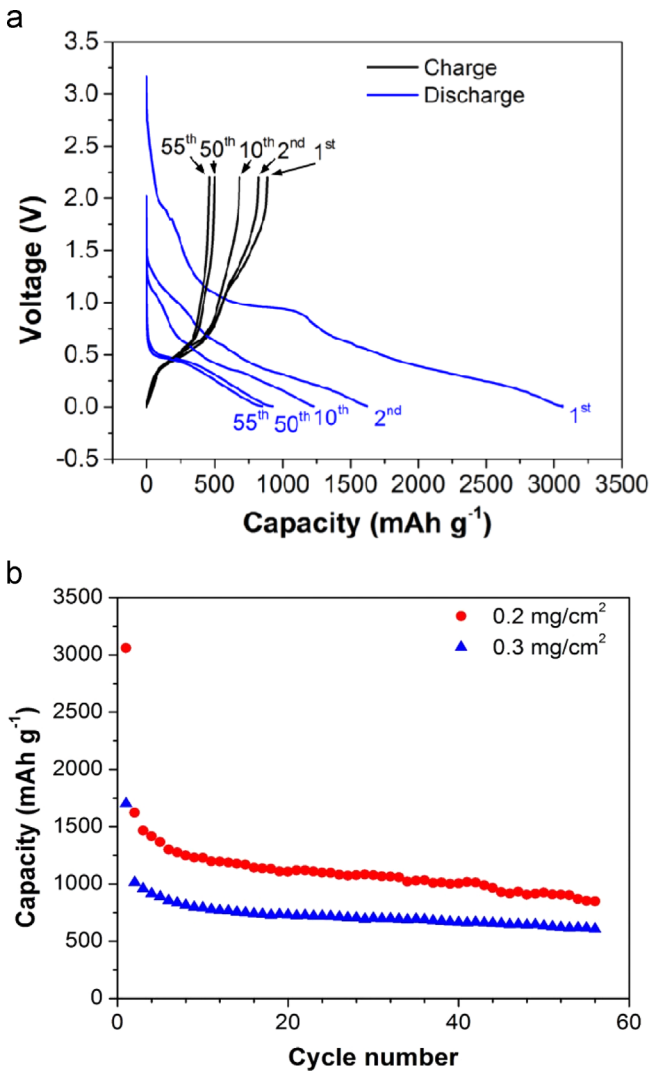

Fig. 10. Galvanostatic curves a) and discharge capacity vs. cycle number b) of tin nanoclusters covered tin oxide nanowires at current density of 100 mA/g.

structures are also known to provide fast charge transport and stress accommodation for lithium ion batteries. In spite of these advantages, tin oxide has been shown to suffer from two major challenges. In addition to mechanical degradation due to volume change (about 250%) (Wachtler et al., 2002), tin oxide also suffers from chemical degradation, i.e., pulverization of tin oxide into tin and non-conducting Li_2O phase. Typically, tin and tin oxide based materials suffer from large irreversible capacity loss in first few cycles and continue to fade in capacity with cycling. Recently, Meduri et al. reported that tin nanocluster on tin oxide nanowires could accommodate the volume expansion and increase the conductivity which is resulted in high reversible capacity of 814 mA h g^{-1} after 100 cycles (Meduri et al., 2009). Based on this concept, the resulting nanowire powders from our synthesis have been treated and tested in lithium ion battery anodes.

The resulting tin oxide nanowire powders from our plasma oxidation technique are partially reduced in a hydrogen microwave plasma reactor to form tin nanocluster on the surface of tin oxide nanowires. The tin nanocluster covered tin oxide nanowires are used as active materials for battery testing. To confirm the durability of the tin oxide nanowire electrodes, all of the electrodes are charged and discharged in the voltage range of 0.005–2.2 V at a current density of 100 mA/g (Fig. 10). The high initial capacity of 1700 mA h g^{-1} is due to the decomposition of electrolyte to form solid electrolyte layer, the reduction of tin oxide to tin, and the insertion of Li ion into tin oxide and tin to form $Li_{4.4}Sn$ alloy. The capacity decreases in first few cycles and remained stable at 614 mA h g^{-1} after 55 cycles. Another set of experiments with lower loading of 0.2 mg/cm^2 shows exceptional high initial capacity of 3059 mA h g^{-1}. The capacity drops quickly in the second cycle to 1623 mA h g^{-1} and remains stable at 848 mA h g^{-1} after 55 cycles at the same current density of 100 mA/g. This is one of the highest capacity retentions obtained for tin oxide. We believe that this high capacity is derived from (1) porous structure of tin oxide which provide high electrode-electrolyte contact area to accommodate the volume change during cycling and to provide pathways for fast transportation of lithium ions and easy accessibility of electrolytes (Mei et al., 2012); (2) lower loading leading to minimum delamination which has been reported as a major issue with tin oxide nanowires (Nguyen et al., 2014).

4. Conclusions

In summary, a simple concept for fast, scalable method is presented and studied for converting tin oxide particles to tin oxide nanowires by mixing it with potassium hydroxide and exposing to an atmospheric microwave plasma reactor. The reaction time scales have been found to be on the order of few tens of

seconds to a minute which makes this technique highly scalable. A production capacity of 300 g per hour can be obtained by a simple lab-scale roll-to-roll setup. A systematic set of experiments revealed the presence of intermediate phase ($K_2SnO_3 \cdot H_2O$) formation which could be held responsible for the observed one-dimensional growth. Further acid wash and annealing of $K_2SnO_3 \cdot H_2O$ allowed for formation of porous tin oxide nanowires. The resulting porous tin oxide nanowires showed a high reversible capacity of 848 mA h g^{-1} after 55 cycles at a current density of 100 mA/g.

Acknowledgment

Authors gratefully acknowledge the Conn Center for Renewable Energy Research for facilities and access to characterization equipment. This material is based upon work supported by the National Science Foundation under Cooperative Agreement no. 1355438.

Appendix A. Supplementary material

Supplementary data associated with this article can be found in the online version at http://dx.doi.org/10.1016/j.ces.2016.03.008.

References

Beltrán, A., Andrés, J., Longo, E., Leite, E.R., 2003. Thermodynamic argument about SnO_2 nanoribbon growth. Appl. Phys. Lett. 83 (4), 635–637.
Cabanas, A., Darr, J.A., Lester, E., Poliakoff, M., 2000. A continuous and clean one-step synthesis of nano-particulate CeZrO solid solutions in near-critical water. Chem. Commun. 11, 901–902.
Chandra, D., Mukherjee, N., Mondal, A., Bhaumik, A., 2008. Design and synthesis of nanostructured porous SnO_2 with high surface areas and their optical and dielectric properties. J. Phys. Chem. C 112 (23), 8668–8674.
Cheng, B., Russell, J.M., Shi, Zhang, L., Samulski, E.T., 2004. Large-scale, solution-phase growth of single-crystalline SnO_2 nanorods. J. Am. Chem. Soc. 126 (19), 5972–5973.
Chung, C.-C., Chung, T.-W., Yang, T.C.K., 2008. Rapid synthesis of titania nanowires by microwave-assisted hydrothermal treatments. Ind. Eng. Chem. Res. 47 (7), 2301–2307.
Dai, Z.R., Gole, J.L., Stout, J.D., Wang, Z.L., 2002. Tin oxide nanowires, nanoribbons, and nanotubes. J. Phys. Chem. B 106 (6), 1274–1279.
Davide, M., Sankaran, M., 2010. Microplasmas for nanomaterials synthesis. J. Phys. D: Appl. Phys. 43 (32), 323001.
Derrien, G., Hassoun, J., Panero, S., Scrosati, B., 2007. Nanostructured Sn–C Composite as an advanced anode material in high-performance lithium-ion batteries. Adv. Mater. 19 (17), 2336–2340.
Gubbala, S., Russell, H.B., Shah, H., Deb, B., Jasinski, J., Rypkema, H., Sunkara, M.K., 2009. Surface properties of SnO_2 nanowires for enhanced performance with dye-sensitized solar cells. Energy Environ. Sci. 2 (12), 1302–1309.
Hui, H., Tan, O.K., Lee, Y.C., Tse, M.S., Guo, J., White, T., 2006. Effects of plasma treatment on the growth of SnO_2 nanorods from SnO_2 thin films. Nanotechnology 17 (3), 743.
Jian, J.K., Chen, X.L., Wang, W.J., Dai, L., Xu, Y.P., 2003. Growth and morphologies of large-scale SnO_2 nanowires, nanobelts and nanodendrites. Appl. Phys. A 76 (2), 291–294.
Kolmakov, A., Potluri, S., Barinov, A., Menteş, T.O., Gregoratti, L., Niño, M.A., Locatelli, A., Kiskinova, M., 2008. Spectromicroscopy for addressing the surface and electron transport properties of individual 1-D nanostructures and their networks. ACS Nano 2 (10), 1993–2000.
Kumar, V., Kim, J.H., Jasinski, J.B., Clark, E.L., Sunkara, M.K., 2011. Alkali-assisted, atmospheric plasma production of titania nanowire powders and arrays. Cryst. Growth Des. 11 (7), 2913–2919.
Liu, Z., Zhang, D., Han, S., Li, C., Tang, T., Jin, W., Liu, X., Lei, B., Zhou, C., 2003. Laser ablation synthesis and electron transport studies of tin oxide nanowires. Adv. Mater. 15 (20), 1754–1757.
Martinez, C.J., Hockey, B., Montgomery, C.B., Semancik, S., 2005. Porous tin oxide nanostructured microspheres for sensor applications. Langmuir 21 (17), 7937–7944.
Meduri, P., Pendyala, C., Kumar, V., Sumanasekera, G.U., Sunkara, M.K., 2009. Hybrid tin oxide nanowires as stable and high capacity anodes for Li-ion batteries. Nano Lett. 9 (2), 612–616.
Mei, L., Li, C., Qu, B., Zhang, M., Xu, C., Lei, D., Chen, Y., Xu, Z., Chen, L., Li, Q., Wang, T., 2012. Small quantities of cobalt deposited on tin oxide as anode material to improve performance of lithium-ion batteries. Nanoscale 4 (18), 5731–5737.
Mozetič, M., Cvelbar, U., Sunkara, M.K., Vaddiraju, S., 2005. A method for the rapid synthesis of large quantities of metal oxide nanowires at low temperatures. Adv. Mater. 17 (17), 2138–2142.
Nguyen, T.Q., Thapa, A.K., Vendra, V.K., Jasinski, J.B., Sumanasekera, G.U., Sunkara, M.K., 2014. High rate capacity retention of binder-free, tin oxide nanowire arrays using thin titania and alumina coatings. RSC Adv. 4 (7), 3312–3317.
Ostrikov, K., Neyts, E.C., Meyyappan, M., 2013. Plasma nanoscience: from nano-solids in plasmas to nano-plasmas in solids. Adv. Phys. 62 (2), 113–224.
Ostrikov, K., Levchenko, I., Cvelbar, U., Sunkara, M., Mozetic, M., 2010. From nucleation to nanowires: a single-step process in reactive plasmas. Nanoscale 2 (10), 2012–2027.
Qin, L., Xu, J., Dong, X., Pan, Q., Cheng, Z., Xiang, Q., Li, F., 2008. The template-free synthesis of square-shaped SnO_2 nanowires: the temperature effect and acetone gas sensors. Nanotechnology 19 (18), 185705.
Wachtler, M., Winter, M., Besenhard, J.O., 2002. Anodic materials for rechargeable Li-batteries. J. Power Sources 105 (2), 151–160.
Wang, Y., Lee, J.Y., Deivaraj, T.C., 2004. Controlled synthesis of V-shaped SnO_2 nanorods. J. Phys. Chem. B 108 (36), 13589–13593.
Wang, Y., Jiang, X., Xia, Y., Solution-Phase, A., 2003. Precursor route to polycrystalline SnO_2 nanowires that can be used for gas sensing under ambient conditions. J. Am. Chem. Soc. 125 (52), 16176–16177.
Winter, M., Besenhard, J.O., 1999. Electrochemical lithiation of tin and tin-based intermetallics and composites. Electrochim. Acta 45 (1–2), 31–50.
Zhang, D.-F., Sun, L.-D., Xu, G., Yan, C.-H., 2006. Size-controllable one-dimensinal SnO_2 nanocrystals: synthesis, growth mechanism, and gas sensing property. Phys. Chem. Chem. Phys. 8 (42), 4874–4880.
Zhang, H., Tan, Z., Xu, P., Oh, K., Wu, R., Shi, W., Jiao, Z., 2011. Preparation of SnO_2 nanowires by solvent-free method using mesoporous silica template and their gas sensitive properties. J. Nanosci. Nanotechnol. 11 (12), 11114–11118.
Zhou, J.X., Zhang, M.S., Hong, J.M., Yin, Z., 2006. Raman spectroscopic and photoluminescence study of single-crystalline SnO_2 nanowires. Solid State Commun. 138 (5), 242–246.